DESIGN, DEVELOPMENT AND TEST OF THE MAGNETS FOR PAL-XFEL*

Hyung Suck Suh, Bongi Oh, Dong Eon Kim, Heung-Sik Kang, Hong-Gi Lee, In Soo Ko, Ki-Hyeon Park, Moo Hyun Cho, Sang-Bong Lee, Seong Hun Jeong, Young-Gyu Jung
PAL, Pohang, Republic of Korea

Abstract

PAL-XFEL is now being constructed with the goal of 0.1 nm hard X-ray in Pohang, Korea. As the first phase we will construct 10 GeV linac, one hard X-ray and one soft X-ray beamlines which require 6 different families of 46 dipole magnets, 11 families of 209 quadrupole magnets, and 3 families of 48 corrector magnets. We have designed these magnets with considering the efficient production and the proper power supplies. This paper describes an outline of the design and test results of the magnets until now.

INTRODUCTION

The PAL(Pohang Accelerator Laboratory)-XFEL is a 0.1-nm hard X-ray FEL project starting from 2011. Three hard X-ray and two soft X-ray branches are planned. As the first phase of this project, one hard X-ray (HX1) and one soft X-ray (SX1) which consist of 51 dipole and 209 quadrupole magnets will be constructed [1].

We have designed all magnets on our own by using OPERA and ANSYS codes [2, 3]. Every magnet is designed to maintain the maximum temperature rise of coils below 20 K for 120% of the nominal currents. In the process of the design, it was helpful to parameterize the main variables of the magnets in a spread sheet for easy estimation by changing some parameter. Now we are manufacturing and testing the magnets. Two Hall probe measurement benches were used to measure the magnetic field for the dipole magnets and the quadrupole magnets respectively.

DIPOLE MAGNETS

The dipole magnets were classified into six kinds according to the pole gap, the effective magnetic length, and the maximum magnetic field. The results of the classification are listed in Table 1.

Most dipole magnets have the same pole gaps of 30 mm except D6 of 15 mm for the self-seeding. D1, D2, and D4 have H-type core shape, and D3, D6, and D7 have C-type. All dipole magnets of D1~D6 for the bunch compressor, the chicane, and the self-seeding have the trim coils with 1% of the main field.

The pole profiles of magnets are optimized by the small bumps at the tip of the pole for the field uniformity. The requirements for the field uniformity are different from each magnet.

Table 1: The Families of Dipole Magnets (D5 was replaced with D2.)

Family	Magnetic length [m]	Max. field [T]	Qty	Position
D1	0.20	0.80	6	BC1
D2	0.70	1.00	19	BC2,BC3, BAS1
D3	1.44	1.30	11	BAS2,3,4
D4	0.17	0.312	4	Laser Heater
D6	0.30	0.485	4	Self seeding
D7	0.75	1.164	2	Tune-up dump

We have tested all prototype dipole magnets. Most magnets satisfied the field requirements. But D1 and D7 didn't satisfy the field uniformity slightly. We have calculated the magnetic field by using B-H table of Chinese low carbon steel (DT4), and manufactured magnets by using the same materials. But a little difference between the calculated and measured field uniformities has arisen. So we used shims (10x10 mm^2 wide, 1mm thick, steel plates) to improve the field uniformity. The shims were placed on the chamfer sides of front and end sides of lower and upper poles. Figure 1 shows the field distribution of FEM model and the magnetic field measurement scene of D1.

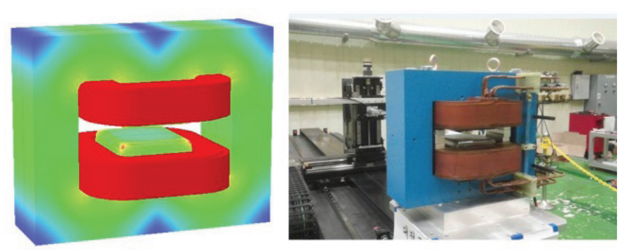

Figure 1: D1 dipole magnet (Left: magnetic field distribution of FEM model, Right: magnetic field measurement by Hall probe).

The field uniformities of D1 are shown in Figure 2, where the calculated one is drawn with a green dashed line, measured without shims with a blue dash-dot line, and measured with shims with a red line. The requirement of the 3-dimensional field uniformity is less than 1.0E-4 for |x| < 17 mm, and less than 5.0E-4 for |x| < 41 mm. And we confirmed that the field uniformities of field integral along straight line are very similar to that along the curved orbit.

ISBN 978-3-95450-134-2

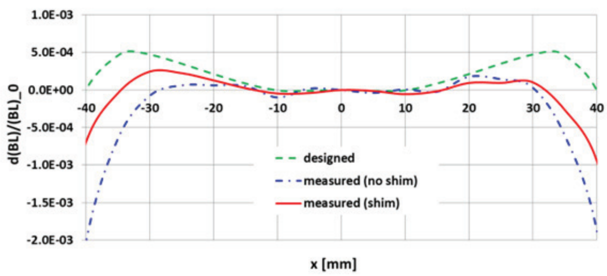

Figure 2: Magnetic field uniformity of D1 dipole magnet (green dashed line: designed, blue dash-dot line: measured without shim, red solid line: measured with shim), $\Delta(BL)/(BL)_0 < 5.0E\text{-}4$ for $|x| < 41$ mm.

The laminated cores are used for the magnets D2 and D3 which quantities are more than 10 magnets, and the solid cores are used for the rest of the dipole magnets which quantities are less than 10.

We measured D2 dipole magnet also. Figure 3 shows the magnetic field distribution of FEM model and the magnetic field measurement scene. Figure 4 shows the field uniformity of calculated and measured field integral. The requirement of the 3-dimensional field uniformity is less than 1.0E-4 for $|x| < 16$ mm, and less than 5.0E-4 for $|x| < 22$ mm.

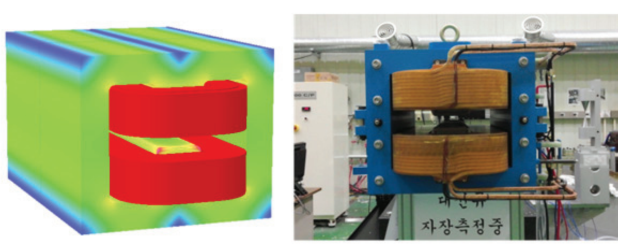

Figure 3: D2 dipole magnet (left: magnetic field distribution of FEM model, right: magnetic field measurement).

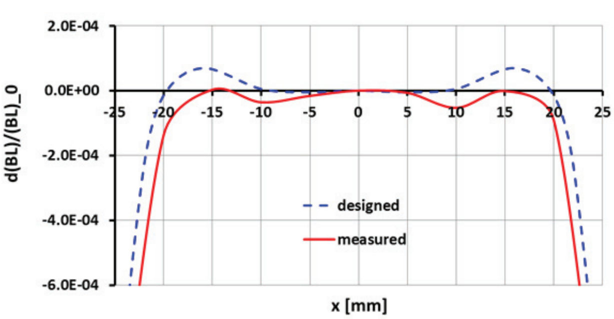

Figure 4: Field uniformity of D2 dipole magnet (blue dashed line: calculated, red line: measured), $\Delta(BL)/(BL)_0 < 5.0E\text{-}4$ for $|x| < 22$ mm.

QUADRUPOLE MAGNETS

The quadrupole magnets were classified into 11 kinds according to the aperture diameter, the effective length, and the maximum field gradient. The results of the classification are listed in Table 2.

Some quadrupole magnets (Q1, Q2, Q3, Q6, and Q9) have the horizontal and vertical steering fields for the bunch compressors and the inter-undulator.

Table 2: The Families of Quadrupole Magnets

Family	Aperture diameter [mm]	Magnetic length [m]	Max. gradient [T/m]	Qty
Q1	30	0.065	15	20
Q2	30	0.13	25	60
Q3	30	0.18	25	18
Q4	44	0.20	25	6
Q5	22	0.40	35	14
Q6	16	0.13	40	31
Q7	80	0.50	18	3
Q8	22	0.25	30	19
Q9	16	0.08	32	18
Q10	44	0.50	25	4
Q11	44	0.10	10	16

The multipole components were calculated by using an equation, the radial component: $B_r(r_0,\varphi) = \Sigma_n \{A_n \sin(n\varphi) + B_n \cos(n\varphi)\}$, where r_0 is the reference radius that is the good field radius. All magnets are optimized to have the relative multipole components less than 1.0E-4 in 3D calculations. Figure 5 shows the half pole contour. In this figure, the o-m line follows along an ideal hyperbola, the m-n is a straight line and a curve after n point. We could satisfy the multipole requirements by manipulating the position and the length of the straight section.

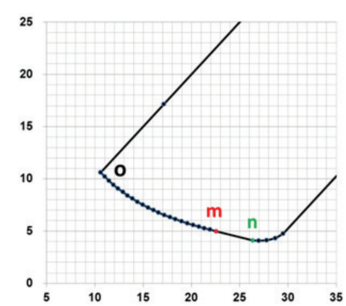

Figure 5: The half pole of quadrupole magnet.

The indirect cooling system (heat sink) for the quadrupole magnets (Q1, Q2, Q3, Q5, Q6, Q8, and Q9) was adopted. Figure 6 shows the cross section of the conductor and the temperature distribution of quadrupole magnet Q2. We used the effective thermal conductivity: $1/k_{eff} = \Sigma v_i/k_i$ for the turn insulation and the ground insulation, where v_i is the volume fraction.

We have tested nine families of quadrupole magnets with a hall probe, and confirmed the field qualities and the temperature rises satisfied the requirements (see Table 3) [4].

ISBN 978-3-95450-134-2

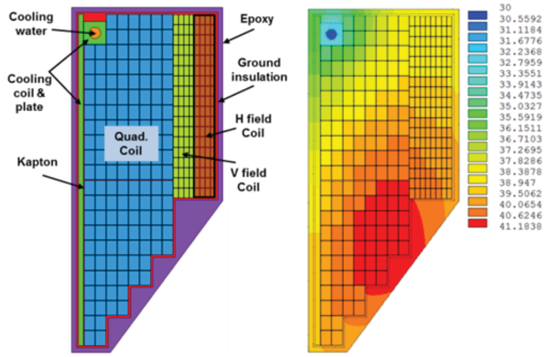

Figure 6: The conductor cross section and the temperature distribution of quadrupole magnet Q2 with a heat sink.

Table 3: Temperature Rise of Quadrupole Magnets

Magnets	Calculated temperature rise [K]	Measured temperature rise [K]
Q1	2	3
Q2	11	15
Q3	11	10
Q4	17	12
Q5	10	15
Q7	12	4
Q8	10	12
Q10	12	9
Q11	2	1

We measured the magnetic field of quadrupole magnets by only Hall probe. Figure 7 shows the field distribution of FEM model and the field measurement scene of Q8 quadrupole magnet. There is a little discrepancy of the field gradient integral of quadrupole magnets by about 2%. Figure 8 shows the field gradient profile of Q8, where the blue dash line is a calculated one and the red line is a measured one. We can see a stacking status of the laminated core by measuring field along the center line of a quadrupole magnet. The field integral would be zero in the ideal quadrupole magnet.

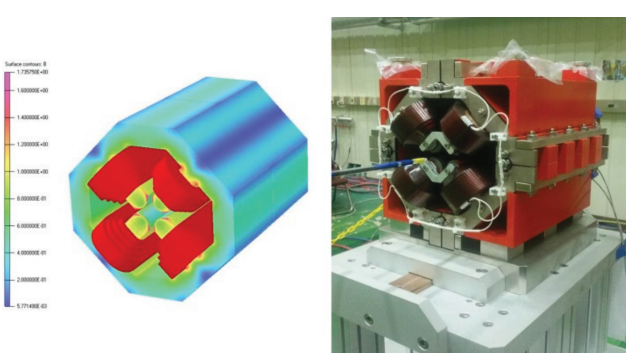

Figure 7: FEM model and field measurement scene of a quadrupole magnet Q8.

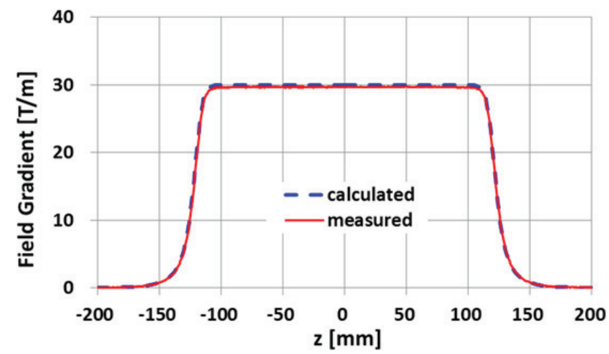

Figure 8: The field gradient profile of Q8 quadrupole magnet.

We have tested all quadrupole magnets of Q1, Q2, Q3, Q5, and Q8. Figures 9 and 10 show the relative field gradient deviations. All quadrupole magnets are excited by the individual power supplies.

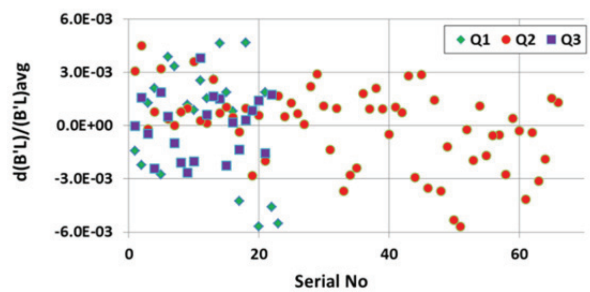

Figure 9: The relative field gradient deviations of Q1, Q2, and Q3 quadrupole magnets.

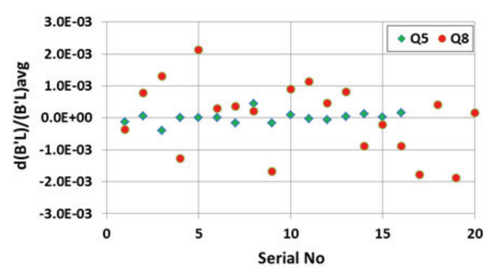

Figure 10: The relative field gradient deviations of Q5, and Q8 quadrupole magnets.

CORRECTOR MAGNETS

The dipole magnets and the quadrupole magnets for the chicanes and the beam analysing have the trim coils or the horizontal/vertical steering coils respectively. Beside these, we prepared the independent corrector magnets of three families of 50 magnets.

Figure 11 shows the corrector magnets, where the right drawing is for the corrector magnets for the undulator, that have an air core in order to maintain no remanent field. Table 4 shows the main parameter of corrector magnets.

ISBN 978-3-95450-134-2

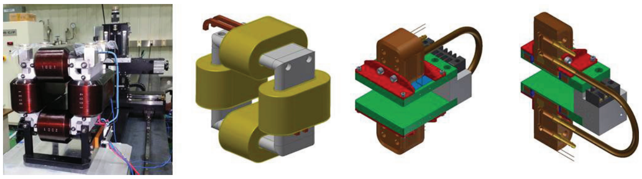

Figure 11: Corrector magnets (left: C1 and C2, right: corrector for undulator).

Table 4: The Main Parameters of Corrector Magnets

Corrector type	C1	C2	C3
Core	iron	iron	iron
Cooling type	air	heat sink	air
Field integral [Gcm]	5000	5000	500
Whole magnet length [mm]	295	144	54
Current density [A/mm^2]	1.1	2.6	0.7
Temperature rise [K]	7	12	9
Quantity(+spare)	36	6	8

CONCLUSION

When we classified the magnets and determined the coil and core sizes, we should consider the connection condition of magnets in series or stand alone, the electrical properties of magnets, and the number of cooling circuit. If the number of cooling circuits is increased in order to reduce the temperature rise, then the magnets become more complicate with the risk of leakage.

We have designed all magnets, and are testing magnets now. Also we confirmed the flow rates of the cooling water that were almost same with estimated ones, and the temperature rises of coils that were below 15 K. Magnetic capabilities of all the magnets have satisfied the requirements till now.

REFERENCES

[1] Heung-Sik Kang, “Current Status of PAL-XFEL Project”, IPAC’13, Shanghai, China (2013).
[2] Vector Fields Software, http://www.cobham.com
[3] ANSYS, http://www.ansys.com
[4] Jack T. Tanabe, “Iron Dominated Electromagnets”, 2005, pp. 113-126

ISBN 978-3-95450-134-2